Microanalysis with Ionization-Loss Electrons

39

CHAPTER PREVIEW

In the previous two chapters we've described how to acquire an energy-loss spectrum and have also given you some idea of the information in such spectra. Most importantly, there are elemental composition data which can be extracted primarily from the high-loss ionization edges. In this chapter we'll examine how to get this information and quantify it. As we've already indicated, the prime use for these kind of data is light-element microanalysis, where EELS complements XEDS. First we'll remind you of the experimental variables over which you have control, because these are rather critical. Then we'll discuss how to obtain a spectrum and what it should look like for microanalysis. Next, we'll discuss the various quantification routines which, in principle, are just as straightforward as those for XEDS but in practice require a rather more sophisticated level of knowledge to carry them out successfully. Finally, we'll say a bit about spatial resolution and minimum detectability, although these topics aren't as important in EELS as they are in XEDS.

D. B. Williams et al., *Transmission Electron Microscopy*

Microanalysis with Ionization-Loss Electrons

39

39.1. CHOICE OF OPERATING PARAMETERS

Perhaps a major reason why EELS is not as widespread as XEDS is the relative complexity of the experimental procedure and the number of variables which you have to define before you can get started. EELS is not yet a "turn-key" operation so you cannot simply place your specimen under the beam, switch on the spectrometer and the computer, and acquire a spectrum. This is in marked contrast to the situation in XEDS, where the high degree of software control means that the XEDS system is almost invariably ready to go when you push the "acquire" button. Furthermore, as you'll see, little useful information is present in the acquired EELS spectrum unless your specimen is very thin. Disko (1986) succinctly summarized the important experimental variables. We've already told you back in Chapter 37 how to control most of these factors. In this chapter, we'll go through all the parameters and indicate reasonable values for each.

- *Beam energy E_0:* It's probably best to use the highest E_0, unless doing so causes displacement damage or surface sputtering. A higher E_0 does reduce the scattering cross section and so you get reduced edge intensity. However, as E_0 increases, the plural-scattering background intensity falls faster than the edge intensity and so the ionization-edge signal-to-background increases and this is useful. The increase in signal-to-background varies with the particular edge but it is never a strong variation; so while we make a lukewarm recommendation to use the highest kV, it's not a good reason to justify purchasing an IVEM.
- *Convergence semiangle α:* You know how to control α with the C2 aperture and/or the C2 lens, but α is only important in the quantification process if it is larger than β. So if you operate in TEM image or diffraction mode with a broad parallel beam, rather than STEM mode, you can ignore any effects of α; otherwise, use the correction factor we give in Section 39.7.
- *Beam size and current:* You control these factors by your choice of electron source, C1 lens, and C2 aperture. As usual, the beam size is important in limiting the spatial resolution in STEM mode, and the beam current controls the signal intensity. You have to make the same compromise between improved spatial resolution and loss of signal intensity, or vice versa, as we discussed at some length in Chapter 36 for XEDS.
- *Specimen thickness:* The specimen must be thin because then the plural-scattering contributions to the spectrum are minimized and quantification is most straightforward.

> Making your specimen as thin as possible is the most important part of EELS.

If your specimen is too thick, then you'll have to use deconvolution procedures to remove the effects of plural scattering. So we'll tell you how to determine the thickness from your spectrum and how to decide if you need to deconvolute the spectrum.

- *Collection semiangle β:* You know from Section 37.4 how to measure β in all operating modes. If you need lots of intensity and are happy with limited spatial resolution, use TEM-image mode with no objective aperture ($\beta \sim 100$ mrad). A small spectrometer entrance aperture would provide better energy resolution at the same time. If you want a small β to prevent contributions to the spectrum from high-angle scattering, use diffraction mode (TEM or STEM) and a small spectrometer entrance aper-

ture for good energy resolution. In the STEM case you also get good spatial resolution.

> Remember that a 5-mm entrance aperture gives β ~5 mrad at a camera length of ~800 mm.

Generally, for microanalysis β ~1–10 mrad is fine, so long as it's less than the Bragg angle for your particular specimen and orientation; but for EELS imaging, which we discuss in Section 40.3, 100 mrad may be necessary.

- *Energy resolution:* ΔE is limited by your electron source, assuming you've focused the spectrum. In a SEELS, the slit width can control ΔE. Microanalysis and imaging do not require the best ΔE and ~5 eV will generally suffice. You really only need the best ΔE for ELNES, and plasmon-shift studies, both of which are somewhat esoteric pursuits. Use an FEG source and a PEELS if you want to do this kind of thing.
- *Energy-loss range and spectrum dispersion:* The full spectrum extends out to the beam energy E_0, but the useful portion only extends to about 1 keV. Above this energy loss, the intensity is very low, and microanalysis by XEDS is both easier and more accurate, although arguably a little less sensitive. So you rarely need to collect a spectrum above about 1 keV and therefore, with a minimum of 1024 channels in the MCA display, 1 eV/channel is always a good starting point. You can easily select a higher display resolution if you want to look at a more limited region of the spectrum or if you want to see detail with $\Delta E < 1$ eV.
- *Signal processing:* In SEELS, remember that your two choices (in which the spectral intensity is determined by the total current on the scintillator) are analog processing or single electron counting. You should collect the high-intensity, low-loss portion of the spectrum in analog mode and the lower-intensity, high-loss region in single-electron mode. The change in counting mode is most conveniently made at the same point in the collection process as the gain change. Set this point around 50–100 eV, well above the plasmon range but at lower $\mathcal{E}$ than most ionization edges. There is no equivalent of this variable in PEELS.
- *Dwell time:* In SEELS, typical dwell times are in the range from 10 ms to 1 s per channel, depending on the number of channels in the spectrum and the intensity necessary to extract the analytical result. Because the magnetic prism is not very stable, it is unwise to collect spectra for periods longer than a few minutes. If more counts are required you should sum several spectra (see below), each recorded over a limited time range, with intermediate checks on the calibration. In PEELS, you set the dwell time (or integration time) such that the maximum intensity in the spectrum doesn't saturate the photodiode array, i.e., stay below 16,000 counts per acquisition in the most intense channel and sum as many spectra as you need to give sufficient counts for analysis.
- *Number of sweeps:* It is better in both SEELS and PEELS to sum many spectra rather than gather one SEELS spectrum for several minutes, or saturate the PEELS detector. Remember also that each sweep in SEELS should be a reverse scan from high to low energy. Furthermore, if the intense zero loss has to be recorded, several minutes should elapse between each scan to ensure that the scintillator after-glow has subsided to below the normal dark-current output of the detector. In PEELS, multiple acquisitions can give rise to artifacts, as we discussed in Section 38.5.

So now you can see why EELS is not a straightforward turn-key operation. You must have a very good understanding of your TEM and spectrometer optics; be aware that the system is not very stable, needs recalibrating regularly and, PEELS, particularly, is prone to artifacts.

39.2. WHAT SHOULD YOUR SPECTRUM LOOK LIKE?

Before you analyze a particular spectrum, you should check three things:

- Display the zero-loss peak to ensure that the spectrometer is giving you the necessary ΔE, if this is important.
- Look at the low-loss portion of the spectrum; this gives you an idea of your specimen thickness.
- Look for the expected ionization edges. If you can't see any edges, your specimen is probably too thick.

The first of these tasks is not critical, as we noted earlier. Regarding the second task, you'll see in Section 39.5 that, to a first approximation, if the plasmon peak intensity is less than about one-tenth the zero-loss peak, then the specimen is thin enough for microanalysis. Otherwise, you'll

probably have to deconvolute plural-scattering effects from your experimental spectrum. For the third task, you should ideally see a discrete edge on a smoothly varying background, but you need to see at least a change in slope in the background intensity at any expected edge energies. The Gatan ELP program can identify and quantify such hidden peaks (see Section 1.5). If the background intensity is noisy, it will make quantification more difficult.

> An important parameter in determining the quality of your spectrum is the signal-to-background ratio which, in EELS, we call the jump ratio.

This is the ratio of the maximum edge intensity (I_{max}) to the minimum intensity (I_{min}) in the channel preceding the edge onset, as shown in Figure 39.1.

If the jump ratio is above ~5, for the carbon K edge at 284 eV from a standard (< 50 nm thick) carbon film at 100 kV, then your TEM-EELS system is operating satisfactorily. Figure 39.1 is a well-defined edge from a film of amorphous carbon. If you can't get such a jump ratio, then perhaps you need to realign the spectrometer, or find a thinner specimen. The jump ratio should increase with increasing kV.

39.3. QUALITATIVE MICROANALYSIS

As with XEDS, you should always carry out qualitative microanalysis to ensure that you have identified all the features in your spectrum. Then you can decide which edges to use for microanalysis.

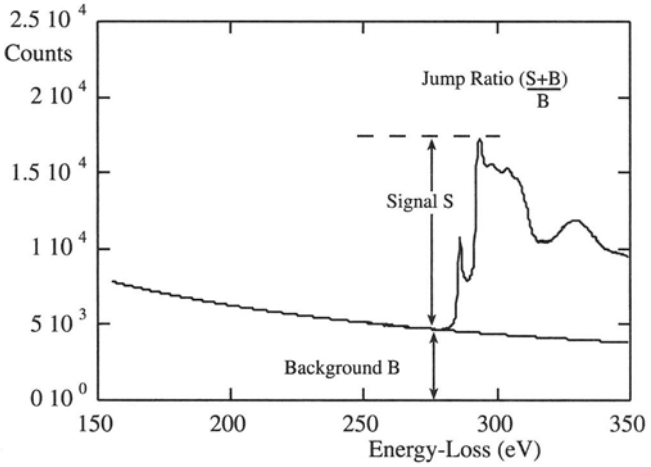

Figure 39.1. Definition of the jump ratio of an ionization edge which should be about 5–10 for the carbon K edge if the EELS is well aligned.

Qualitative microanalysis using ionization edges is very straightforward. Unlike XEDS, there are actually very few artifacts that can be mistaken for an edge. The most prominent artifact that may lead to misidentification is the so-called ghost edge from diode saturation in PEELS spectra (see Section 38.5). So long as you calibrate the spectrum to within 1–2 eV you can unambiguously identify the edge energy.

> We identify the ionization edge as the energy loss at which there is a discrete increase in the slope of the spectrum; this value is the edge onset, i.e., E_C, the critical ionization energy.

You have to be careful here: sometimes you'll see the edge energy defined somewhat arbitrarily half-way up the edge, e.g., at the π^* peak on the front of a C K edge. There is no strict convention, and very often L and M edges do not have sharp onsets anyhow.

Examination of a portion of a spectrum, such as that shown back in Figure 38.6, is usually sufficient to let you draw a definite conclusion about the identity of the specimen, which is BN on a C support film. In addition, it is wise to compare your spectrum with reference spectra from one of several EELS libraries that are available (Zaluzec 1981, Ahn and Krivanek 1983, Colliex 1984).

Remember that there are families of edges (K, L, M, etc.) just as there are families of peaks in X-ray spectra. As a rule of thumb, quantification is equally easy with K and L edges, but the accuracy of K-edge quantification is slightly better. Up to Z = 13 (Al) we usually use K edges, because any L edges occur at very low energy and are masked by the plasmon peak. Above Z = 13 you can use either K or L edges. Sometimes, there is the question of which edge is most visible. The K-edge onset is generally a bit sharper than the L edge, which consists of both the L_2 and L_3 edges and so may be somewhat broader. This is not always the case.

> L edges for Z = 19–28 and 37–45 are characterized by intense near-edge structure, called white lines. M edges for Z = 55–69 have similar intense lines.

These white lines, which we first saw back in Figure 38.9, are so named because of their appearance in early, photographically recorded energy-loss spectra; more details are given in Section 40.1. If you have to use the M, N, or O edges without any white lines, you should know that they are very broad, with an ill-defined threshold, and quantification is only possible with standards, as we'll see shortly.

The energy-loss spectrum clearly does not lend itself to a quick "semiquantitative" analysis, as we can do with XEDS. For example, the spectrum in Figure 38.6 comes from equal numbers of B and N atoms, but the intensities in the B and N edges are markedly different. This difference arises because of the variation in ionization cross section with $\mathcal{E}$, the strongly varying nature of the plural-scattering background, and the edge shape, which causes the C and N K edges to ride on the tails of the preceding edge(s).

Example

Sometimes, qualitative analysis is all that you need to do. Figure 39.2A and Figure 39.2B show images and spectra from two small precipitates in an alloy steel. The spectra show a Ti L_{23} edge in both cases, and C and N K edges in Figure 39.2A and Figure 39.2B, respectively. It does not take much effort to deduce that the first particle is TiC because it is the only known carbide of Ti, but the nitride could be either TiN or Ti_3N. To determine which of the two it is, you have to carry out full quantification, which we'll discuss shortly. You should note that such clear discrimination between TiC and TiN in Figure 39.2 would be difficult using windowless XEDS, because the energy resolution is close to the separation of the Ti L (452 eV) and the N K (392 eV) X-ray peaks. In addition, the DPs from both phases are almost identical, so this problem is a perfect one for EELS.

39.4. QUANTITATIVE MICROANALYSIS

To quantify the spectrum, you have to extract intensity in the ionization edge(s) by removing the plural-scattering background and integrating the intensity (I) in the edge.

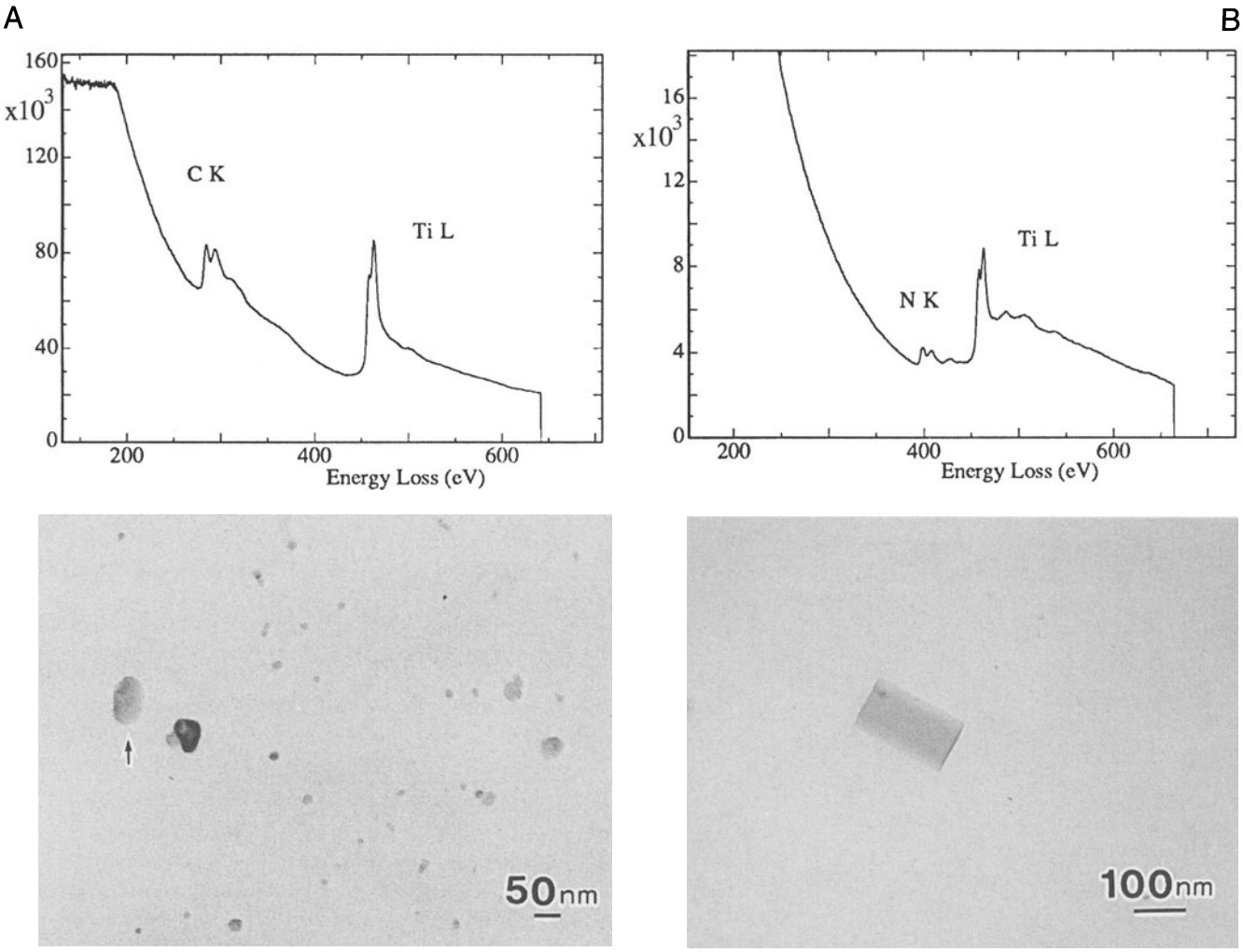

Figure 39.2. Images of small precipitates in a stainless steel specimen, and the corresponding ionization edges showing qualitatively the presence of Ti, C, and N. Thus the precipitates can be identified as (A) TiC and (B) TiN, respectively.

Then you have to determine the sensitivity factor, that is, you need to determine the number of atoms N responsible for I. This sensitivity factor is called the "partial ionization cross section." We'll see that it plays a similar role to the k_{AB} factor in X-ray microanalysis. If you go back and look at Figure 38.5, you'll see how an ionization edge is built up from several contributions. The process of quantification in essence involves stripping away (or ignoring) the various contributions until you're left with Figure 38.5A, which contains the single-scattering "hydrogenic" edge intensity.

39.4.A. Derivation of the Equations for Quantification

The equations we use for quantitative analysis have been derived, refined, and applied by Egerton and co-workers. The following derivation is a summary of the full treatment by Egerton (1996), which itself draws on work carried out over the preceding two decades.

We'll assume that we are quantifying a K edge, although the basic approach can be used for all edges. The K-shell intensity above background, I_K, is related to the probability of ionization, P_K, and the total transmitted intensity, I_T

$$I_K = P_K I_T \qquad [39.1]$$

This equation assumes that the intensities are measured over the complete angular range (0–4π sr), which of course is not the case, but we'll correct for this later. In a good thin specimen we can approximate I_T to the incident intensity, neglecting backscatter and absorption effects. Now, this is the important point:

If we assume also that the electrons contributing to the edge have only undergone a single ionization event, then we can easily obtain an expression for P_K

$$P_K = N\sigma_K \exp\left(\frac{t}{\lambda_K}\right) \qquad [39.2]$$

where N is the number of atoms *per unit area* of the specimen (thickness t) that contribute to the K edge. The assumption of a single K-shell ionization event with cross-section σ_K is reasonable, given the large mean free path (λ_K) for ionization losses; but it explains why you have to make thin specimens. It also means that the exponential term is very close to unity, and so

$$I_K \approx N\sigma_K I_T \qquad [39.3]$$

and therefore

$$N = \frac{I_K}{\sigma_K I_T} \qquad [39.4]$$

Thus we can measure the absolute number of atoms per unit area of the specimen simply by measuring the intensity above background in the K edge and dividing it by the total intensity in the spectrum and the ionization cross section. We can easily extend this expression to a spectrum containing two edges from elements A and B, in which case the total intensity drops out and we can write

$$\frac{N_A}{N_B} = \frac{I_K^A \sigma_K^B}{I_K^B \sigma_K^A} \qquad [39.5]$$

Similar expressions apply to L, M edges, etc., and combinations of edges can be used. So you see that if you are quantifying more than one element then you don't need to gather the zero-loss peak, and this makes life much easier for the spectrometer scintillator or diode array.

In both equations 39.4 and 39.5 we assumed that we could accurately subtract the background under the ionization edge and that we know σ. Unfortunately, as you'll see, both background subtraction and determination of σ are nontrivial and limit the accuracy of quantification. We will discuss these points later, but initially we must take account of the practical realities of spectrum acquisition and modify the equations accordingly.

First, you can't gather the whole of the energy-loss spectrum out to the beam energy, E_0, because above 1–2 keV the intensity decreases to a level close to the system noise. Furthermore, while ionization-loss electrons can theoretically have any energy between E_C and E_0, in practice the intensity in the edge falls to the background level within about 100 eV of the ionization threshold, E_C. In addition, the background extrapolation process becomes increasingly inaccurate beyond about 100 eV, and so it is imperative to restrict the integration of spectral intensities to some window, Δ, usually in the range of 20–100 eV. So we modify equation 39.4 to give

$$I_K(\Delta) = N\sigma_K(\Delta) I_T(\Delta) \qquad [39.6]$$

The term $I_T(\Delta)$ is more correctly written as $I_\ell(\Delta)$, where I_ℓ is the intensity of the zero-loss (direct beam) electrons combined with the low-loss electrons over an energy loss window Δ. Only if we have true single scattering can we use I_T, and we'll discuss the conditions for this later.

As we discussed, EELS has the tremendous advantage that the energy-loss electrons are predominantly forward-scattered and so you can easily gather most of the signal. As a result, the technique is inherently far more efficient than XEDS. However, because we cannot physically collect the spectrum over 4π sr, but are limited by our

choice of collection semiangle β, we must further modify the equation and write

$$I_K(\beta\Delta) = N\sigma_K(\beta\Delta)I_\ell(\beta\Delta) \qquad [39.7]$$

The factor $\sigma_K(\beta\Delta)$ is termed the "partial ionization cross section," from this equation, therefore, the absolute quantification for N is given by

$$N = \frac{I_K(\beta\Delta)}{I_\ell(\beta\Delta)\sigma_K(\beta\Delta)} \qquad [39.8]$$

For a ratio of two elements A and B, the low-loss intensity drops out

$$\frac{N_A}{N_B} = \frac{I_K^A(\beta\Delta)\sigma_K^B(\beta\Delta)}{I_K^B(\beta\Delta)\sigma_K^A(\beta\Delta)} \qquad [39.9]$$

We can draw a direct analogy between this equation and the Cliff–Lorimer expression (equation 35.2) used in thin-foil XEDS. In both cases, the composition ratio C_A/C_B or N_A/N_B is related to the intensity ratio I_A/I_B through a sensitivity factor, which we call the k_{AB} factor in XEDS and which in electron spectrometry is the ratio of two partial cross sections, σ^B/σ^A.

Remember that the major assumption in this whole approach is that the electrons undergo *a single scattering event*. In practice, it's difficult to avoid plural scattering, although in very thin specimens the approximation remains valid, if errors of ±10–20% are acceptable. If plural scattering is significant then the spectrum must be deconvoluted, and we will discuss ways to do this in Section 39.6 when we describe the limitations of specimen thickness. You should also note when using the ratio equation that your analysis is a lot better if the two edges are similar in shape, i.e., both K edges or both L edges, otherwise the approximations inherent in equation 39.9 will be less accurate.

In summary then, these equations give us an absolute value of the atomic content of the specimen or a ratio of the amounts of two elements. You have to carry out two essential practical steps:

- The background subtraction to obtain I_K.
- The determination of the partial ionization cross section $\sigma_K(\beta\Delta)$.

So now you can see why it is important to know β.

39.4.B. Background Subtraction

The background intensity comes from plural-scattering events which are usually associated with outer-shell interactions. In the spectrum the background appears as a rapidly changing continuum decreasing from a maximum just after the plasmon peak at about 15–25 eV, down to a minimum at which it is indistinguishable from the instrumental noise, typically when $\mathcal{E} \sim$ 1–2 keV. In addition to the true plural scattering, there is also the possibility of single-scattering contributions to the background from the tails of preceding ionization edges. Because of the complexity of the many combinations of plural-scattering processes, it has not proven possible to model the background from first principles to the same degree that is possible in XEDS using variations on Kramers' Law. There are two ways commonly used to remove the background:

- Curve fitting.
- Using difference spectra.

We'll now describe these in some detail.

Curve Fitting: You select a window δ in the background before the edge onset and fit a curve to the channels. Then you extrapolate the curve over the desired energy window Δ under the edge. This process is shown schematically in Figure 39.3, and experimentally in Figure 39.4.

We assume that the energy dependence of the background has the form

$$I = A\,\mathcal{E}^{-r} \qquad [39.10]$$

where I is the intensity in the channel of energy loss $\mathcal{E}$, and A and r are constants for a particular curve fit. The fitting parameters are only valid over a limited energy range because they depend on $\mathcal{E}$. The exponent r is typically in the

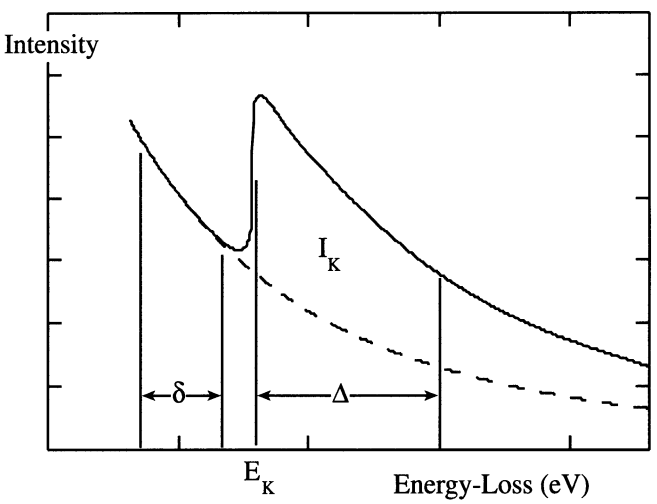

Figure 39.3. The parameters required for background extrapolation and subtraction under an ionization edge. The pre-edge fitting window δ is extrapolated over a post-edge window Δ then subtracted to give the edge intensity I_K.

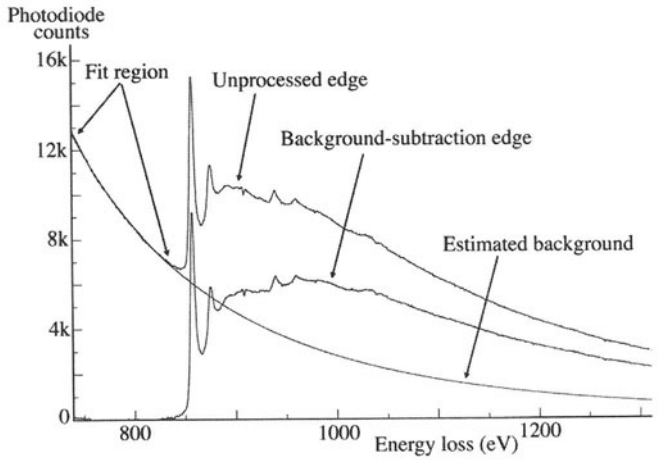

Figure 39.4. A Ni $L_{2,3}$ edge before and after background subtraction. The fit region before the unprocessed edge is extrapolated to give the estimated background, which is then removed, leaving the background-subtracted edge.

range 2–5, but A can vary tremendously. We can see some trends in how r varies. The value of r decreases as:

- The specimen thickness, t, increases.
- The collection semiangle, β, increases.
- The electron energy loss, $\mathcal{E}$, increases.

The fit to the tail of a preceding edge also shows a similar power-law dependence on the plural-scattering background, and may be fitted in a similar manner, i.e., $I = B\mathcal{E}^{-s}$. The energy range δ over which you fit the background should not be <~10 channels, and at most not >~30% of E_K. In practice, however, you might not be able to fit the background over such a wide window if another edge is present within that range.

You should choose the extrapolation window, Δ, such that the ratio of the finish to the start energies, $\mathcal{E}$(finish)/$\mathcal{E}$(start), is <1.5. In Figure 39.4, the extrapolation window (~450 eV) is a little larger than ideal. So, Δ is smaller for lower edge energies. Using larger windows, although improving the statistics of the total edge integration, eventually reduces the accuracy of the final quantification because the fitting parameters A and r are only valid over ~100 eV. If there's a lot of near-edge structure, either use a larger Δ to minimize its effect or avoid it in the extrapolation window, unless the quantification routine can handle it.

Instead of the simple power-law fit, you can use any expression such as an exponential, polynomial, or log-polynomial, so long as it provides a good fit to the background and gives acceptable answers for known specimens. Polynomial expressions can behave erratically if you extrapolate them over a large Δ, so use them cautiously. Generally, the power law seems adequate for most purposes except close to the plasmon peaks ($\mathcal{E}$ <~100 eV). Clearly, the background channels closest to the edge onset will influence the extrapolation most strongly, and various weighting schemes have been proposed. A noisy spectrum will be particularly susceptible to poor fitting, unless some type of weighting is used.

We can judge the "goodness of fit" of a particular power-law expression qualitatively by looking at the extrapolation to ensure that it is heading toward the post-edge background and not substantially under- or over-cutting the spectrum. More quantitatively, we can assign a χ^2, chi-squared, value based on a linear least-squares fit to the experimental spectrum. The least-squares fit can be conveniently tied in with a weighting scheme using the expression

$$\chi^2 = \sum_i \frac{(y - y_i)^2}{y^2} \qquad [39.11]$$

where y_i is the number of counts in the ith channel and $y = \ln_e I$. The squared term in the denominator ensures suitable weighting of the channels close to the edge.

Difference Spectra: You can also remove the background using a first-difference approach (which is equivalent to differentiating the spectra). This method is particularly suited to PEELS since it simply involves taking two spectra, offset in energy by a few eV, and subtracting one from the other. As shown in Figure 39.5, the difference process results in the slowly varying intensity (i.e., background) being reduced to zero and the rapidly varying intensity features (i.e., ionization edges) showing up as classical difference-peaks, similar to what you may have seen in an Auger spectrum. This is the *only* way to remove the background if your specimen thickness changes over the area of analysis, and it also has the advantage that it sup-

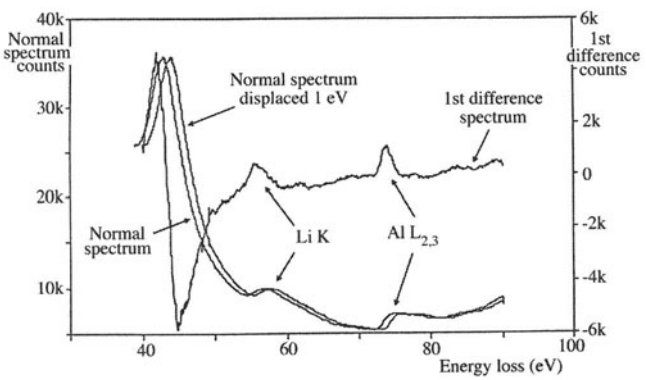

Figure 39.5. First-difference method of background subtraction, showing two PEELS spectra from a specimen of Al-Li displaced by 1 eV and subtracted to give a spectrum in which the background intensity falls to zero and the small Li K and Al $L_{2,3}$ edges are clearly revealed.

presses spectral artifacts common to PEELS, particularly the channel-to-channel gain variation.

Another kind of difference method involves convoluting the experimental spectrum with a filter function. A top-hat filter function, similar to the one we described in Section 35.2 for background subtraction in XEDS, gives a second-difference spectrum which also removes the background but exacerbates some artifacts.

39.4.C. Edge Integration

The edge integration procedure you use depends on how you removed the background. If you used a power-law approach, then remember that there is a limit over which the edge integration window Δ is valid. The value of Δ should be large enough to maximize the integrated intensity, but not so large that the errors in your background extrapolation dominate. Often, the presence of another edge limits the upper end of the integration window. The lower end is usually defined from the edge onset, E_K, but if there is strong near-edge structure, such as in the B K edge or the Ca L_{23} edge, then your integration window should start at an energy above these, unless the quantification schemes can handle fine structure effects (see below). If you subtracted the background using a first-difference approach, then you determine the peak intensity by fitting the experimental spectrum to a reference spectrum from a known standard using multiple least-squares fitting. We'll talk more about this when we discuss deconvolution of spectra.

39.4.D. The Zero-Loss Integral

Remember from equation 39.8 that if you want *absolute* quantification of N, then you have to integrate the low-loss spectrum I_ℓ out to about 50 eV. In a SEELS you should always do this using a reverse scan to avoid any problems with after-glow of the scintillator, and in PEELS you must be careful to integrate for a short enough time so you don't saturate the diode array. If you are doing a ratio, then I_ℓ is not needed (equation 39.9).

39.4.E. The Partial Ionization Cross Section

There are several ways we can determine the partial ionization cross section, $\sigma(\beta\Delta)$, which is the sensitivity factor relating intensity (I) to the number of atoms (N). We either use a theoretical approach or compare the experimental spectra with known standard spectra.

Theoretical Calculation: The most common approach is that due to Egerton (1979, 1981), who produced two short computer programs to model the K- and L-shell partial cross sections. The programs are called SIGMAK and SIGMAL, respectively. They are public domain software and are available in Gatan's ELP software, but the code is also given in Egerton's book.

> The cross sections are modeled by approximating the atom in question to an isolated hydrogen atom with a charge on the nucleus equal to the atomic number Z of the atom, but with no outer-shell electrons.

While at first sight this is an absurd approximation, the approach is tractable because the hydrogen-atom wave function can be expressed analytically by Schrödinger's wave equation, which can be modified to account for the increased charge. Because this treatment neglects the outer-shell electrons, it is best suited to K-shell electrons, and Figure 39.6 shows a comparison between the measured N K-shell intensity and that computed using SIGMAK. As you can see, the SIGMAK hydrogenic model essentially ignores the near-edge and post-edge fine structure (which would be absent in the spectrum from a hydrogen atom), but still gives a very good fit, on average, to the experimental edge. Figure 39.7 compares the Cr L edge with the SIGMAL model. The L-shell fit is almost as good as the K fit, but the white lines are imperfectly modeled. These programs are very widely used since they are simple to understand and easy and quick to apply.

There is another theoretical approach which uses empirical parameterized equations to calculate the terms that modify σ for the effects of β and Δ. Both Joy (1986b) and Egerton (1989) have given relatively simple expressions, amenable to evaluation on a hand-held calculator, which you can look up if you wish. Joy's parameterization approach and the SIGMAK/SIGMAL models give good agreement, as shown in Figure 39.8. There are more com-

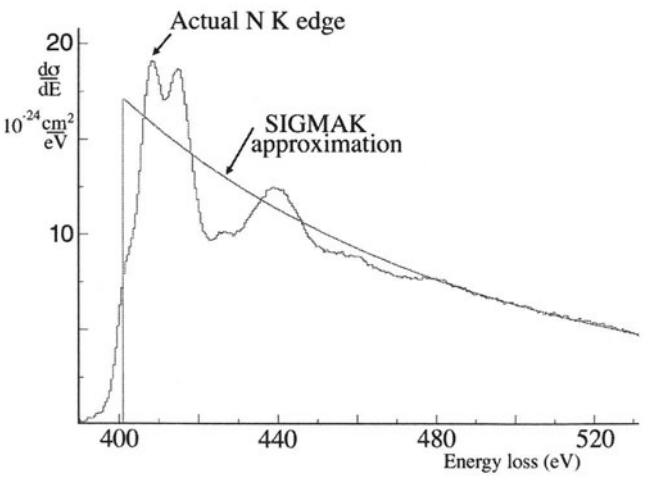

Figure 39.6. Comparison of an experimental N K edge and the hydrogenic fit to the edge using the SIGMAK program.

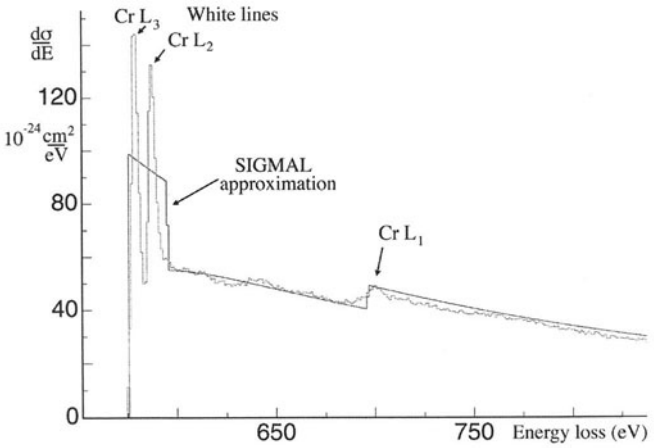

Figure 39.7. Comparison between an experimental Cr $L_{2,3}$ edge and a modified hydrogenic approximation to the edge obtained using the SIGMAL program. The fit makes no attempt to model the intense white lines, but only makes a rough estimate of their average intensity.

plex methods available which calculate the cross section in a more realistic way than the hydrogenic model, e.g., using Hartree–Slater models or atomic-physics approaches, which are better for the more complex L and M edges (Rez 1989). Egerton (1993) has compared experimental and theoretical cross sections, and the M-shell data (which are the worst case) are shown in Figure 39.9. The data are actually plotted in terms of the oscillator strength f (which is a measure of the response of the atom to the incident electron). This term is the integral of the generalized oscillator strength, which is proportional to the differential cross section, so just think of f as proportional to σ. There is still relatively poor agreement between experiment and theory for the M shell, as well as between the atomic and hydrogenic theoretical models. Similar data in Egerton's paper show

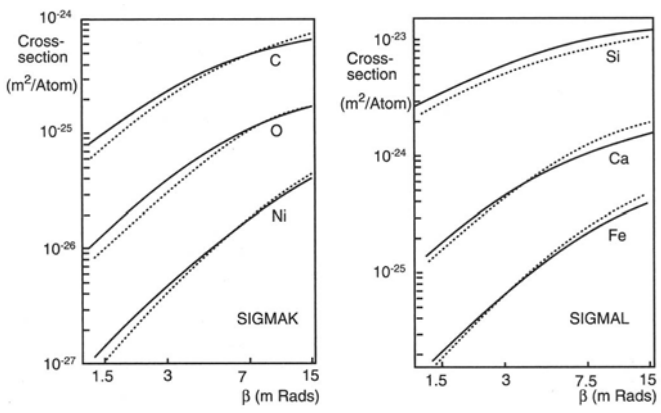

Figure 39.8. Comparison of the SIGMAK and SIGMAL hydrogenic models (full lines) for the ionization cross section with the parametric model (dotted lines).

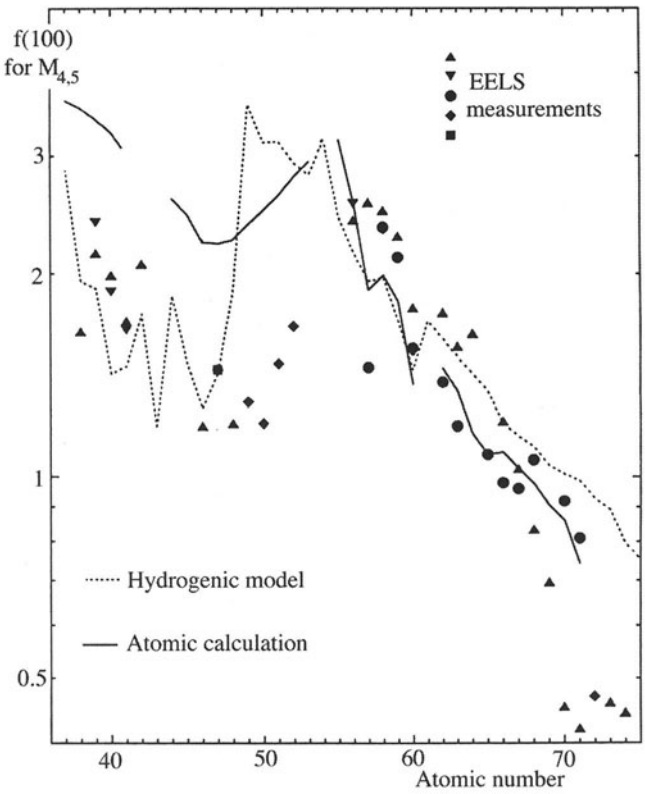

Figure 39.9. Comparison of the experimental and theoretical approaches to determination of the M-shell ionization cross section shown in terms of the variation in the dipole oscillator strength (f) as a function of atomic number. The data points are different experimental measurements, the solid line is a fundamental atomic calculation, and the dotted line is a hydrogenic calculation.

better agreement for K and L shells. These models, while more precise, require substantially longer computing time, but this is fast becoming less of a problem. Given the other sources of error in EELS microanalysis, you rarely need to go to such lengths to obtain a better value of $\sigma(\beta\Delta)$, and you should generally stick with the SIGMAK/L approach for routine quantification.

Experimental Determination: Rather than calculating σ theoretically, you can generate a value experimentally using known standards. This approach is, of course, exactly analogous to the experimental k-factor approach for XEDS quantification in which the cross section is automatically included (along with the fluorescence yield and other factors). It is surprising at first sight that the classical XEDS approach of using standards has not been widely used in EELS, but the reason is obvious when you remember the large number of variables that affect the EELS data. The standard and unknown must have the same thickness and the same bonding characteristic, and the spectra must be gathered under identical conditions; in particular β, Δ, E_0, and t must be the same.

Again, it is the problem of thickness measurement that appears to be the main limitation to improving the accuracy of microanalysis.

Despite these limitations, data are available comparing cross sections of various elements, relative to oxygen (Hofer *et al.* 1988), just as *k* factors are determined relative to Si or Fe. Malis and co-workers (Malis *et al.* 1987, Malis and Titchmarsh 1988) have also produced a large number of experimental cross sections for light-element compounds. It is intriguing to note that the experimental approach appears increasingly popular in EELS, while in XEDS the reverse trend, toward more theoretical modeling of *k* factors, seems to be the case!

The SIGMAK/L programs may introduce large errors when quantifying the lightest metallic elements, Li and Be, so for the most accurate quantification of these elements the standards approach is still the best.

Example

In a study of Al-Li alloys (Liu and Williams 1989), a homogeneous sample of Al-12.7 at.% Li was used as a standard; t was determined from the relative intensities of the first plasmon peak and the zero-loss peak. The integrated intensity ratio for the Li K/Al L_{23} edges was determined after background subtraction to be 0.106±0.006. This number was the average of six separate spectra, and the errors were based on a student t analysis at the 95% confidence limit. From equation 39.9, the Li/Al partial-cross-section ratio was calculated to be 1.37±0.07. An Al-Li specimen containing an intermetallic of unknown Li content was then examined and 13 spectra obtained which gave an average Li K/Al L_{23} intensity ratio of 0.188±0.009. Combining this ratio with the partial ionization cross section and substituting back into equation 39.9 gives the composition of the intermetallic as Al-20.5±1 at.%Li. This result and others are given in Figure 39.10, which shows the low-Li portion of the Al-Li phase diagram, determined through direct Li composition measurements. For comparison, the partial ionization cross section was also determined from the SIGMAK/L programs, and the ratio was 0.969, ~30% less than that obtained using the standard. While this is a large difference compared to most SIGMAK/L calculations, it still sounds a note of caution against unquestioning use of the calculated cross sections.

In summary, there are two approaches to the determination of $\sigma(\beta\Delta)$: theoretical calculation and experimental measurement. In contrast to XEDS, the theoretical approaches dominate. There is good evidence that, particularly for the lighter elements for which EELS is best suited, the simple and quick hydrogenic model is usually adequate. However, for the heavier elements, where the M shell is used for analysis, tedious experimental data are still the best option. Of course, for such elements it is probably better to revert to XEDS analysis anyhow.

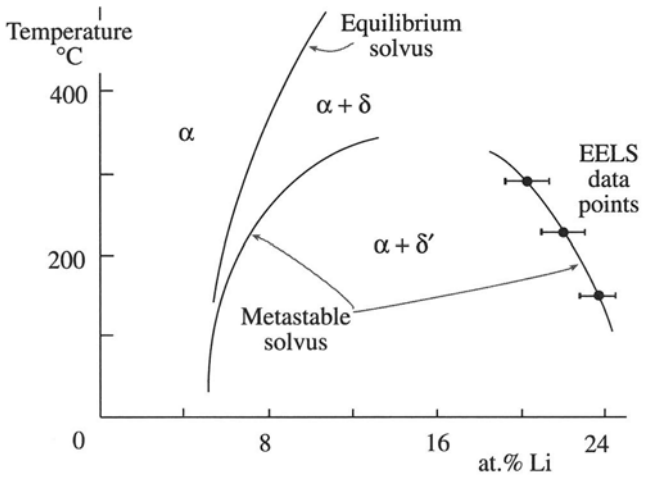

Figure 39.10. The Al-Li phase diagram determined by EELS, showing a variation in the Li content of the metastable Al_3Li (δ′) phase as the temperature is raised. The equilibrium phases are α (Al-Li) solid solution and δ (Al-Li) intermetallic.

So now we're in a position where we have all the data needed to solve the quantification equations. However, our assumption all along has been that the spectra were the result of single scattering and we neglected plural scattering. Now in practice there will *always* be some plural-scattering contribution to the ionization edges.

The combination of a plasmon interaction and an ionization will show up as a bump about 15–25 eV past the onset of the edge.

This effect is shown schematically back in Figure 38.5F and, if you look ahead, in Figure 39.15. So how do we go about correcting for this? We can either make our specimens so thin that plural scattering is negligible, or we can deconvolute the spectra. The former approach is possible, but you have to be lucky or exceptionally skilled at specimen thinning. The latter approach is mathematically simple, but can be misleading if not done properly, so we will need to examine deconvolution in more detail; but let's look at how we determine t because EELS offers us a simple method for this.

39.5. MEASURING THICKNESS FROM THE ENERGY-LOSS SPECTRUM

There is thickness information in the energy-loss spectrum since the amount of all inelastic scatter increases with

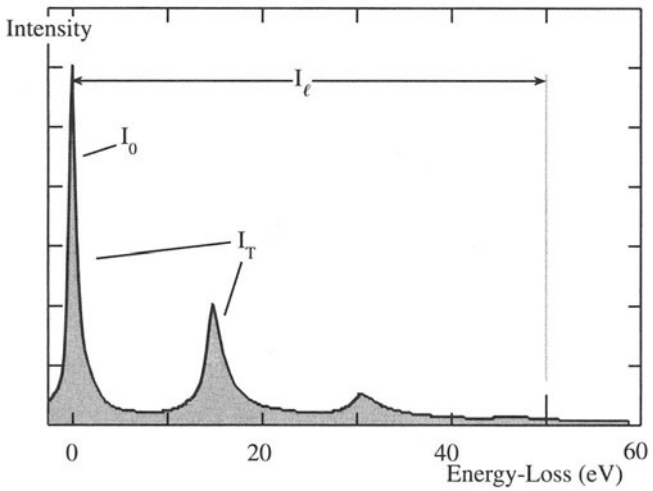

Figure 39.11. Definition of the zero-loss intensity I_0, the total intensity I_T, and the low-loss (I_ℓ) intensity required for thickness determination.

specimen thickness. In principle we have to measure the intensity under the zero-loss peak (I_0) and ratio this to the total intensity in the spectrum (I_T), as defined in Figure 39.11. But in practice the intensity in the EELS spectrum falls so rapidly with increasing energy loss that we can reasonably approximate I_T to the intensity in the low-loss portion of the spectrum I_ℓ, out to about 50 eV. The relative intensity of the zero loss and the total intensity is governed by the average mean free path (λ) for energy losses up to 50 eV, and thus

$$t = \lambda \ln\left(\frac{I_\ell}{I_0}\right) \qquad [39.12]$$

All we need is to determine λ for the specimen, and we get this from a parameterization based on many experimental measurements (see Malis *et al.* 1988). The expression is

$$\lambda = \frac{106\, F E_0}{\left\{\mathcal{E}_m \ln\left(\frac{2\beta E_0}{\mathcal{E}_m}\right)\right\}} \qquad [39.13]$$

where λ is in nm, E_0 in keV, β in mrad, F is a relativistic correction factor, and $\mathcal{E}_m$ is the average energy loss in eV which, for a material of average atomic number Z, is given by

$$\mathcal{E}_m = 7.6\, Z^{0.36} \qquad [39.14]$$

The relativistic factor (F) is given by

$$F = \frac{\left\{1 + \frac{E_0}{1022}\right\}}{\left\{1 + \left(\frac{E_0}{511}\right)^2\right\}} \qquad [39.15]$$

You can easily store these equations in the TEM computer or in your calculator and they give an accuracy for t of better than ±20%.

If indeed your specimen is so thin that only single scattering occurs, then you can use a similar expression but assume that the only significant scatter was a single plasmon event. Thus

$$t = \lambda_P \frac{I_P}{I_0} \qquad [39.16]$$

where λ_P is the plasmon mean-free path (see Table 38.2), I_P is the intensity in the first (and only) plasmon peak, and I_0 is the intensity in the zero-loss peak.

The method has advantages over other thickness measurement techniques in that you can apply it to any specimen, amorphous or crystalline, over a wide range of thicknesses.

If plural scattering is significant, then your quantification results become unreliable.

A typical ball-park figure is that, if the intensity in the first plasmon peak is greater than one-tenth the zero-loss intensity, then your specimen is too thick.

Another way of saying this is that, if $t > 0.1\lambda_P$, then errors >~10% are expected, as shown in Figure 39.12. Of course,

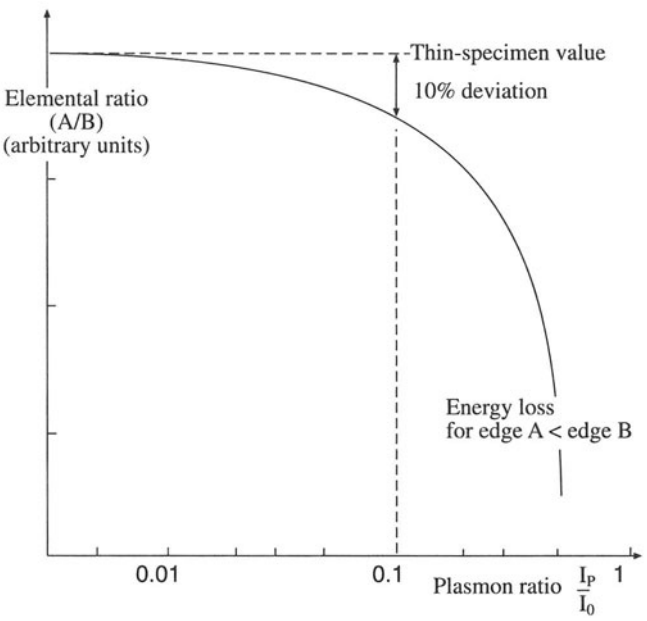

Figure 39.12. The intensity ratio of two ionization edges (A/B) as a function of specimen thickness. The thickness is plotted in terms of the ratio of the plasmon to the zero-loss intensity (I_P/I_0). The intensity ratio is affected significantly when I_P is above about 0.1 I_0.

one way round this problem is to use very thin foils, but often you can't produce thin enough specimens. Murphy's law says that the area you're interested in will usually be too thick. Then you have to deconvolute the spectra to make the single-scattering assumption valid.

39.6. DECONVOLUTION

We saw back in Figure 38.5 that the effect of plural scattering is to add intensity to the ionization edge, mainly as a result of combined inner- and outer-shell losses.

> We can represent the experimental ionization edge as a true single-scattering (hydrogenic) edge convoluted with the plasmon, or low-loss, spectrum.

The aim of the deconvolution process therefore, as shown schematically in Figure 39.13, is to extract the single-scattering intensity distribution. We'll describe two methods, the Fourier-Log and the Fourier-Ratio, which are both based on the work of Egerton *et al.* (1985), and both methods are incorporated in the Gatan ELP proprietary software. Strictly speaking, the deconvolution should be carried out in both the energy dimension and the angular dimension, but in practice all the routines ignore the angular dimension; this simplification introduces a small systematic error into any deconvolution. The error is usually <10% up to typical energy losses below about 1 keV, so we can usually ignore it. A smaller β increases the deconvolution error, since the plural-scattered electrons have a wider angular distribution and so more of them are excluded as β decreases.

The *Fourier-Log* method removes the effects of plural scattering from the whole spectrum. The technique describes the spectrum in terms of the sum of individual scattering components, i.e., the zero-loss (elastic contribution) plus the single-scattering spectrum plus the double-scattering spectrum, etc. Each term is convoluted with the "instrument response function," which is a measure of how much the spectrometer degrades the generated spectrum; in the case of a PEELS, this is the point-spread junction we described in Section 37.3. The Fourier transform of the whole spectrum (F) is then given by

$$F = F(0)\exp\left(\frac{F(1)}{I_0}\right) \qquad [39.17]$$

where $F(0)$ is the transform of the elastic contribution, $F(1)$ is the single-scattering transform, and I_0 is the zero-loss intensity. So to get the single-scattering transform you take logarithms of both sides, hence the name of the technique.

Extracting the single-scattering spectrum would ideally involve an inverse transformation of $F(1)$, but this results in too much noise in the spectrum. There are various ways around this problem, the simplest of which is to approximate the zero-loss peak to a delta function. After deconvolution, you can subtract the background in the usual way, prior to quantification.

The danger of this approach is that you may introduce artifacts into the single-scattering spectrum. In particular, any gain change in a SEELS spectrum must be removed or not incorporated in the original spectrum at all. Despite the assumptions and approximations, the net result of deconvolution is often an increase in the ionization edge jump ratio. This improvement is important when you are attempting to detect small ionization edges from trace elements, or the presence of edges in spectra from thick specimens. An example of Fourier-Log deconvolution is shown in Figure 39.14.

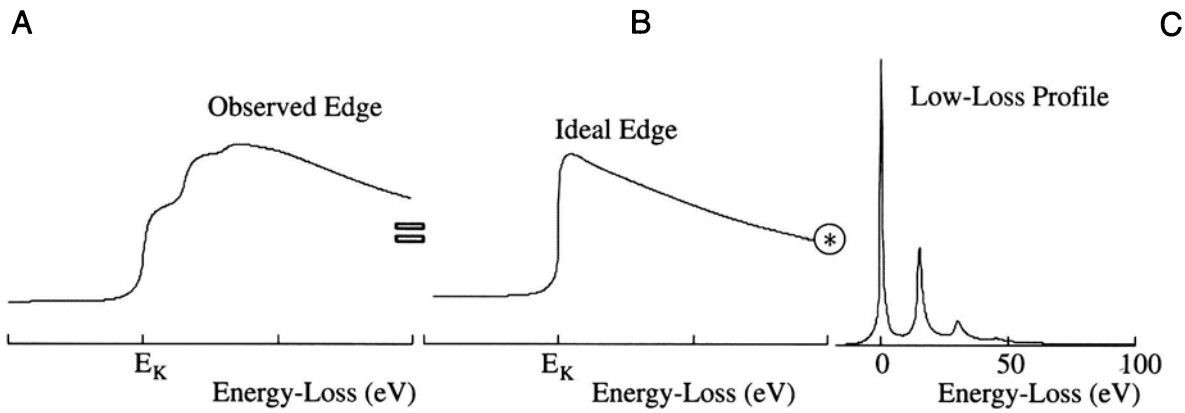

Figure 39.13. The contribution of plural scattering to the experimentally observed ionization edge intensity profile (A) is determined by the convolution of the ideal single-scattering ionization edge (B) with the low-loss plasmon region (C).

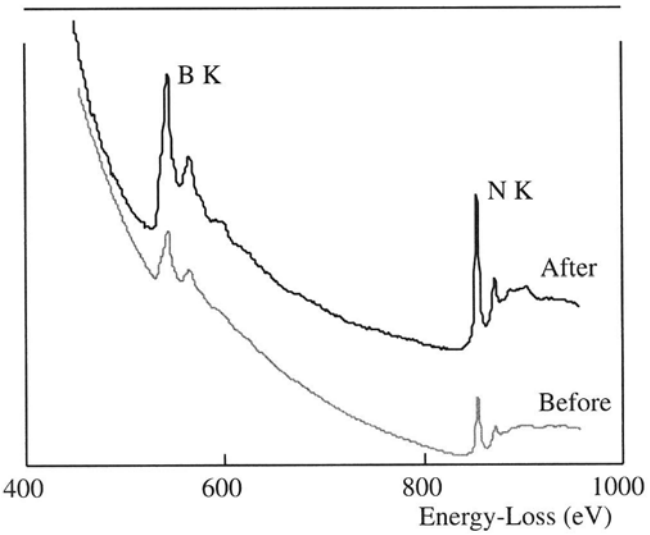

Figure 39.14. A spectrum from a thick crystal of BN before and after Fourier-Log deconvolution. The jump ratio is increased in the deconvoluted spectrum, which is displaced vertically for clarity.

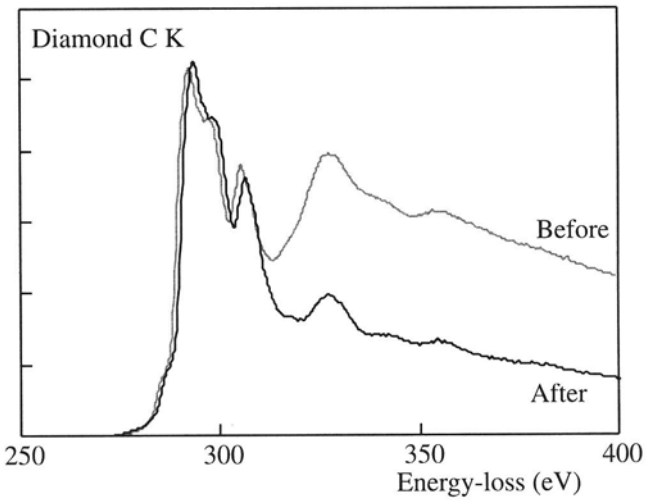

Figure 39.15. A carbon K edge from a thick specimen before and after Fourier ratio deconvolution. The plural scattering plasmon contribution to the post-edge structure is removed.

The *Fourier-Ratio* technique approximates the experimental spectrum to the ideal single-scattering spectrum, convoluted with the low-loss spectrum. We define the low-loss portion of the spectrum as the region up to ~50 eV, including the zero-loss peak, but before the appearance of any ionization edges. So we can now write

$$F' = F(1).F(P) \qquad [39.18]$$

where F' is the Fourier transform of the experimental intensity distribution around the ionization edge and $F(P)$ is the Fourier transform of the low-loss (mainly plasmon) spectrum. In this equation, therefore, the instrument response is approximated by the low-loss spectrum rather than the zero-loss peak. If we rearrange equation 39.18 to give a ratio (hence the name of the technique)

$$F(1) = \frac{F'}{F(P)} \qquad [39.19]$$

we now obtain the single-scattering distribution by carrying out an inverse transformation. In contrast to the Fourier-Log technique, you must subtract the background intensity before you deconvolute. Again, to avoid the problem of increased noise, it is necessary to multiply equation 39.19 by the transform of the zero-loss peak. Figure 39.15 shows a carbon K edge before and after Fourier-Ratio deconvolution.

Multiple Least-Squares Fitting: If your specimen is not uniformly thin, Fourier techniques won't work. Then you should use multiple least-squares (MLS) fitting of convoluted reference spectra (Leapman 1992). A single-

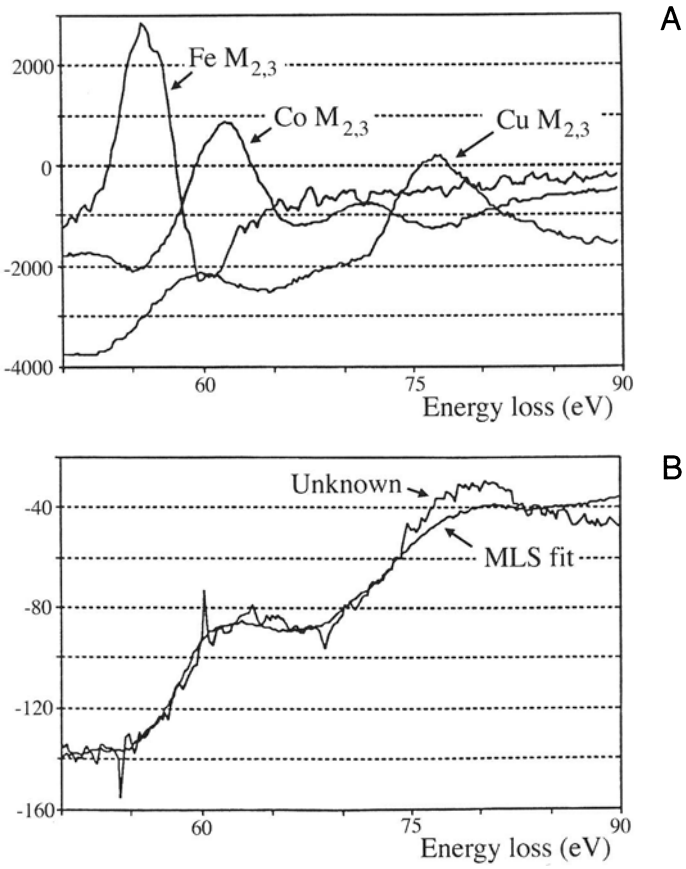

Figure 39.16. (A) Three first-difference M edge reference spectra from Fe, Co, and Cu. (B) MLS fit of the reference spectra superimposed on a low-energy portion of an experimental spectrum from an intermetallic particle in a Cu alloy showing the good fit that can be obtained.

scattering reference spectrum $R_0(\mathcal{E})$ in the region of the edge to be quantified is convoluted with the first plasmon-loss portion of the unknown spectrum (P) and the resultant spectrum $R_1(\mathcal{E}) = P^*R_0(\mathcal{E})$ is used to generate several reference spectra ($R_2(\mathcal{E}) = P^*R_1(\mathcal{E})$, etc.). These reference spectra are then fitted to the experimental spectrum using MLS routines and specific fitting parameters are obtained. An experimental set of Fe, Co, and Cu reference spectra is shown in Figure 39.16A and the actual fit to part of the experimental spectrum from an intermetallic in a Cu-Be-Co alloy is shown in Figure 39.16B.

In summary, to quantify ionization-loss spectra you need a single-scattering spectrum, which can be approximated if you have very thin specimens or generated by deconvolution of your experimental spectrum. It is arguable that all spectra should be deconvoluted prior to quantification, but the uncertain effects of the possible errors introduced by deconvolution mean that you should do this cautiously. Often you'll find it useful to deconvolute the point-spread junction from all PEELS spectra, since this sharpens the edge onset and any ELNES intensity variations.

> Always check the validity of the deconvolution routine by applying it to spectra from a known specimen obtained over a range of thickness.

39.7. CORRECTION FOR CONVERGENCE OF THE INCIDENT BEAM

If you're working in STEM mode to get high spatial resolution, then it is possible that the beam-convergence angle, 2α, may introduce an error into your quantification. When 2α is equal to or greater than 2β, convergence effects can limit the accuracy because the experimental angular distribution of scattered electrons will be wider than expected. Therefore, you have to convolute the angular distribution of the ionization-loss electrons with the beam-convergence angle. Joy (1986b) proposed handling this through a simple equation which calculates the effective reduction (R) in $\sigma(\beta\Delta)$ when α is greater than β

$$R = \frac{\left[\ln\left(1 + \frac{\alpha^2}{\theta_{E^2}}\right)\beta^2\right]}{\left[\ln\left(1 + \frac{\beta^2}{\theta_{E^2}}\right)\alpha^2\right]} \qquad [39.20]$$

where θ_E is the characteristic scattering angle. So you can see that if α is small (particularly if it is smaller than β), then R is $<<1$ and the effect of beam convergence is negligible.

39.8. THE EFFECT OF THE SPECIMEN ORIENTATION

In crystalline specimens, diffraction may influence the intensity of the ionization edge. This effect may be particularly large if your specimen is oriented close to strong two-beam conditions. Both X-ray emission and ionization-loss intensity can change because of electron channeling effects close to the Bragg condition. At the Bragg condition the degree of beam–specimen interaction increases, compared with zone-axis illumination where no strong scatter occurs; the energy-loss processes behave similarly. This phenomenon, known as the Borrmann effect in XEDS (see Section 35.8) is not important for low-energy edges, but intensity changes of a factor of two have been reported for Al and Mg K edges (Taftø and Krivanek 1982). The use of large α minimizes the problem in XEDS, but beam-convergence effects are themselves a problem in EELS. The easiest way to avoid orientation effects is simply to operate under kinematical conditions and stay well away from any bend centers or bend contours, just as in XEDS.

39.9. SPATIAL RESOLUTION

In contrast to the situation in XEDS, beam spreading is not a major factor in determining the source of the EELS signal and so the many factors that influence beam spreading are mainly irrelevant. The spectrometer only collects those

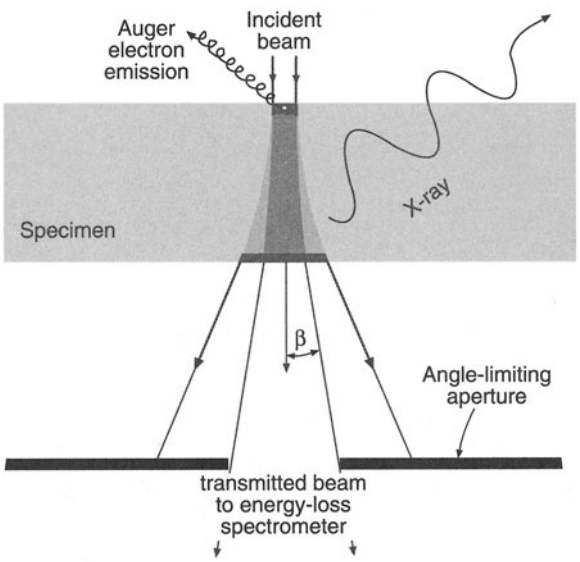

Figure 39.17. The effect of the spectrometer collection angle is to limit the contribution to the spectrum from high-angle scattered electrons, thus ensuring a high spatial resolution signal.

electrons emanating from the specimen in a narrow cone, as shown in Figure 39.17. Therefore, energy-loss electrons that are elastically scattered through large angles are excluded from contributing to your spectrum. Remember that for XEDS these same high-angle electrons would still generate X-rays some distance from the incident probe position, and these X-rays would be detected by XEDS.

In the absence of a contribution from beam spreading, the spatial resolution of ionization-loss spectrometry depends on the mode of analysis:

- The factor controlling the resolution in STEM mode, or in a probe-forming mode on a TEM, is mainly the size of the probe; we can easily get data with probe sizes <10 nm, and <1 nm with more difficulty.
- When we operate in TEM mode, the spatial resolution is a function of the selecting aperture, i.e., the spectrometer entrance aperture and its effective size at the plane of the specimen.

In TEM mode, chromatic aberration usually limits the spatial resolution, as we showed back in Section 37.4.B. We know that the EELS signal isn't affected much by beam spreading and we can easily limit the source of the signal to a few nanometers with an FEG. So, there have been correspondingly fewer studies of the limits of spatial resolution. Most work on defining the spatial resolution has been pursued in France by Colliex and co-workers, e.g., Colliex (1985). Because the primary factor when operating in STEM mode (especially with an FEG) is the incident-probe diameter, we have to be concerned about the problems of spherical aberration broadening the probe (Colliex and Mory 1984). So you must be careful in your selection of the beam-defining aperture. We discussed this topic in detail in the section on the spatial resolution of XEDS.

One factor that we often consider in EELS, but ignore in XEDS (although it occurs in X-ray generation also), is the phenomenon of delocalization.

> Delocalization is the ejection of an inner-shell electron by the passage of a high-energy electron some distance from the atom.

If you are physics oriented and want to read more about this, see Muller and Silcox (1995). The scale of this wave-mechanical effect is small, in the range 2–5 nm, and it is inversely proportional to the energy loss. So it appears that, except in rare cases, delocalization will not limit the spatial resolution; the practical factors such as probe aberrations, signal-to-background in the EELS signal, and damage are much more important. So we can conclude that spatial resolution for EELS will be somewhat better than for XEDS and experiments seem to indicate that this indeed is the case (Colliex 1985). In fact, in certain zone-axis misorientations, it appears that the (FEG) electron beam, if it is <1 nm, can be localized to individual rows of atoms, producing atomic-level spatial resolution (see Figure 40.5C and Browning *et al.* 1993).

39.10. DETECTABILITY LIMITS

The detectability limits for ionization-loss spectrometry are governed by the same factors as we discussed for XEDS. Therefore, the inverse relationship with spatial resolution also applies. Clearly we have to optimize several factors:

- The edge intensity.
- The signal-to-background ratio (jump ratio).
- The efficiency of signal detection.
- The time of microanalysis.

EELS has an inherently higher efficiency than XEDS, but a correspondingly poorer signal-to-background because of the higher background in the spectrum. Joy (1986a) has attempted to compare the two techniques in some detail and calculations based on a thermionic source. He concluded that the MMF for EELS would be of the order of 1–10% in a Si foil 50 nm thick; this value is somewhat worse than the experimental data for XEDS in similar specimens. Leapman and Hunt (1991) have argued that in most situations, PEELS is more sensitive to the presence of small amounts of material than XEDS.

The time of collection, which strongly influences the detectability limit, is particularly dependent on whether serial or parallel collection is used. Colliex (1985) reckons

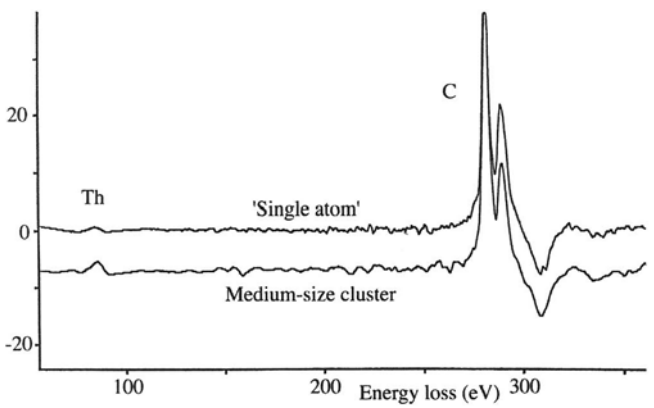

Figure 39.18. First-difference spectra showing the detection of a small cluster and a single atom of Th on a carbon support film.

that a tenfold improvement in all EELS performance criteria is to be expected if parallel collection is used. The best results, combining sensitivity and spatial resolution, will be obtained with an FEG. Krivanek *et al.* (1991) used an FEG DSTEM, parallel detection, and sophisticated data processing to detect the presence of single atoms of Th on thin carbon films, as shown in Figure 39.18. While this is a most favorable analysis situation because of high Z of the atoms and the low average Z of the support film, the result still shows clearly the superiority of the best possible EELS microanalysis over XEDS, which cannot yet detect single atoms.

In conclusion, microanalysis using ionization edges, while considerably more difficult to perform than XEDS, appears to offer both improved spatial resolution and analytical sensitivity. Parallel collection is significantly better than serial collection in both aspects. As was the case for XEDS, an FEG source is required for the best performance.

CHAPTER SUMMARY

The ionization edges can be used to give quantitative elemental analyses from all the elements in the periodic table using a ratio equation. Beware, however, of the many experimental variables you have to define for your TEM, the PEELS, and the specimen. Compared to XEDS there have been very few quantitative analyses or composition profiles measured using EELS.

To use Egerton's ratio equation:

- You have to subtract the background using a power law or MLS approach. The former is easier.
- Integrate the edge intensity. That's straightforward.
- Then you have to determine the partial ionization cross section $\sigma_K(\beta\Delta)$. This is more difficult.
- Calculate $\sigma_K(\beta\Delta)$ with SIGMAK and SIGMAL for most K and L edges.
- For M edges and for the lightest elements (e.g., Li), use known standards.

The difficulty with using standards is that the specimen thickness has to be the same as the unknown and the standard also has to have the same bonding type as the "unknown." This is often impossible, although specimen thicknesses can be deduced directly from the low-loss spectrum intensity. The biggest limitation to quantification is that, ideally, your specimens have to be less than one mean-free path in thickness (typically < 50 nm) otherwise deconvolution routines are needed, which can introduce artifacts on their own.

Spatial resolution and minimum detectability are better than XEDS. Single-atom detection has been demonstrated.

REFERENCES

General References

Egerton, R.F. (1996) *Electron Energy-Loss Spectroscopy in the Electron Microscope,* 2nd edition, Plenum Press, New York.

Joy, D.C. (1986a) in *Principles of Analytical Electron Microscopy* (Eds. D.C. Joy, A.D. Romig Jr., and J.I. Goldstein), p. 249, Plenum Press, New York.

Joy, D.C. (1986b) in *Principles of Analytical Electron Microscopy* (Eds. D.C. Joy, A.D. Romig Jr., and J.I. Goldstein), p. 277, Plenum Press, New York.

Maher, D.M. (1979) in *Introduction to Analytical Electron Microscopy* (Eds. J.J. Hren, J.I. Goldstein, and D.C. Joy), p. 259, Plenum Press, New York.

Williams, D.B. (1987) *Practical Analytical Electron Microscopy in Materials Science,* 2nd edition, Philips Electron Optics Publishing Group, Mahwah, New Jersey.

Specific References

Ahn, C.C. and Krivanek, O.L. (1983) *EELS Atlas,* Gatan, Inc., 780 Commonwealth Drive, Warrendale, Pennsylvania 15086.

Browning, N.D., Chisholm, M.F., and Pennycook, S.J. (1993) *Nature* **366**, 143.

Colliex, C. (1984) *Advances In Optical and Electron Microscopy* **9** (Eds. R. Barer and V. E. Cosslett), p. 65, Academic Press, New York.

Colliex, C. (1985) *Ultramicroscopy* **18**, 131.

Colliex, C. and Mory, C. (1984) *Quantitative Electron Microscopy* (Eds. J.N. Chapman and A.J. Craven), p. 149, SUSSP Publications, Edinburgh, Scotland.

Disko, M.M. (1986) in *Microbeam Analysis-1986* (Eds. A.D. Romig Jr. and W.F. Chambers), p. 429, San Francisco Press, San Francisco, California.

Egerton, R.F. (1979) *Ultramicroscopy* **4**, 169.

Egerton, R.F. (1981) in *Proc. 39th EMSA Meeting* (Ed. G.W. Bailey), p. 198, Claitors, Baton Rouge, Louisiana.
Egerton, R.F. (1989) *Ultramicroscopy* **28**, 215.
Egerton, R.F. (1993) *Ultramicroscopy* **50**, 13.
Egerton, R.F., Williams, B. G., and Sparrow, T.G. (1985) *Proc. Roy. Soc.* **A398**, 395.
Hofer, F., Golob, P., and Brunegger, A. (1988) *Ultramicroscopy* **25**, 181.
Krivanek, O.L., Mory, C., Tence, M., and Colliex, C. (1991) *Microsc. Microanal. Microstruct.* **2**, 257.
Leapman, R.D. (1992) in *Transmission Electron Energy Loss Spectrometry in Materials Science* (Eds. M.M. Disko, C.C. Ahn, and B. Fultz), p. 47, TMS, Warrendale, Pennsylvania.
Leapman, R.D. and Hunt, J.A. (1991) *Microsc. Microanal. Microstruct.* **2**, 231.
Liu, D.R. and Williams, D.B. (1989) Proc. Roy. Soc. London **A425**, 91.
Malis, T., Rajan, K., and Titchmarsh, J.M. (1987) in *Intermediate Voltage Electron Microscopy* (Ed. K. Rajan), p. 78, Philips Electron Optics Publishing Group, Mahwah, New Jersey
Malis, T. and Titchmarsh, J.M. (1988) in *Electron Microscopy and Analysis–1985* (Ed. G.J. Tatlock), p. 181, Adam Hilger Ltd., Bristol and Boston, Massachusetts.
Malis, T., Cheng, S., and Egerton, R.F. (1988) *J. Electron Microsc. Tech.* **8**, 193.
Muller, D.A. and Silcox, J. (1995) *Ultramicroscopy* **59**, 195.
Rez, P. (1989) *Ultramicroscopy* **28**, 16.
Taftø, J. and Krivanek, O.L. (1982) *Phys. Rev. Lett.* **48**, 560.
Zaluzec, N.J. (1981) in *Analytical Electron Microscopy-1981* (Ed. R.H. Geiss), p. 193, San Francisco Press, San Francisco, California.